FINAL TECHNICAL REPORT

USGS NEHRP AWARD G09AP00079

June 1, 2009 – August 31, 2010

Finding the Path Effect for Shear Waves in the Central U.S. Using Broadband Waveform Inversion

Charles A. Langston

Center for Earthquake Research and Information
University of Memphis
3876 Central Ave., Suite 1
Memphis, TN 38152-3050

Telephone: (901)-678-4869
Fax: (901) 678-4734
Email: clangstn@memphis.edu

October 31, 2011

ABSTRACT

USGS NEHRP AWARD G09AP00079, *3D Finding the Path Effect for Shear Waves in the Central U.S. Using Broadband Waveform Inversion* by Charles A. Langston, Center for Earthquake Research and Information, University of Memphis, 3876 Central Ave., Suite 1, Memphis, TN 38152-3050. Telephone: (901) 678-4869, Fax:(901) 678-4734, Email:clangstn@memphis.edu

The physical basis for distance attenuation in the New Madrid Seismic Zone was investigated through a detailed study of explosion P wave and S wave data obtained from the 2002 Embayment Seismic Excitation Experiment. The data show a distinct anisotropy in distance attenuation for both P and S waves in the range from 0 to 200 km distance. Waves that propagate northward from the 2500 lb Marked Tree, AR, explosion attenuate quickly with distance until a range of about 100 km from the source where high-amplitude, high-phase velocity critical reflections from the boundary between the upper crust and "rift pillow" structure produce high amplitude waves. Propagation southward from the 5000 lb Mooring blast shows less distance attenuation compared to northward propagation. Reflections from the upper crust-lower crust boundary occur but do not significantly increase the amplitude with distance and travel with slower apparent phase velocity than observed for the northward propagation data set. Both sets of data can be explained with a relatively simple geometrical model where the "rift pillow" south of the Reelfoot fault thins by 10 km over a distance of about 70 km southward. This interface has a dip of approximately 8° and is consistent with some previous rift pillow geometrical constructions. Dependence of distance attenuation on 3D crustal structure in the Central U.S. suggests that it will be difficult to predict distance attenuation without dense empirical data sets or without well-controlled seismic experiments to determine crustal structure. There is also a need for efficient 2D and 3D wave propagation codes to model data seismograms with synthetics.

INVESTIGATIONS UNDERTAKEN

This project was seismological in scope and involved the collection, processing, and interpretation of a diverse earthquake and explosion source data set to develop models of shear wave velocity and anelasticity for the central U.S. Table 1 outlines the original proposed research program.

The main change from proposed and executed research concerns the discovery of significant crustal heterogeneity affecting distance attenuation in the Embayment Seismic Excitation Experiment (ESEE) explosion data. Considerable effort was spent in demonstrating the truth of the inferred crustal heterogeneity. Unfortunately, the resulting crustal heterogeneity implied decreased the scope of the present work concerning the modeling of earthquake seismograms since 2D and 3D wave propagation codes would be needed to test structure models against the waveform data. My original assumption was that 1D structure models would be sufficient to match major characteristics of the data. However, results from the well-controlled ESEE data set show that, even in the best of circumstances, 2D waveform methods may be necessary to explain the physical bases of distance attenuation.

Data Collection (complete)
• *USGS Refraction Data from the 1991 Embayment Experiment (IRIS data center)* • *Embayment Seismic Excitation Experiment (ESEE) Temporary Broadband and NM Network Short period and Broadband Data from the 2002 Experiment* • *NM Network Short Period, Broadband, and ANSS data from M3.5 and greater events (Table 2)*
Data Processing
• *Choose appropriate filters to process observed shear wave arrivals in the vertical component and 3 component explosion data* • *Pick shear wave arrival times from all available explosion data* • *Perform instrument corrections and find appropriate bandpass filters for short period, ANSS, and broadband to clearly observe SH waveforms* • *Choose SH waveform attributes (times and amplitudes)* • *Archive processed waveforms and waveform attributes*
Data Modeling/Interpretation
• *Produce shear wave crustal velocity models using ray theoretical methods (e.g. ray theory forward modeling and Weichert-Herglotz inversion)* • *Use existing earthquake source parameters and develop source models for each target earthquake* • *Produce shear wave crustal velocity models using "phase time" and "phase amplitude" inversion*

Table 1 – Summary of the Original Proposed Research Program

Introduction

The attenuation of seismic shear waves with distance is a basic problem in the determination of earthquake shaking hazards (*Kramer*, 1996) and quantification of the earthquake source from observed seismic data (*Hutton and Boore*, 1987). Shear waves are almost always the largest waves important in strong ground motions from sources observed at local and near-regional distances (Δ < 500 km). Recently *Miao and Langston* (2007) determined the parameters for a local magnitude scale appropriate for the New Madrid Seismic Zone (NMSZ) and the central U.S. and found that the distance attenuation curve was significantly different from southern California, Tanzania, and Eastern North America (*Kim*, 1998) (Figure 1).

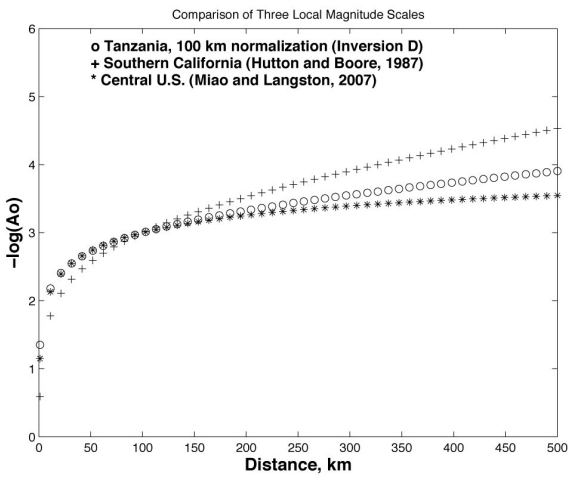

Figure 1 - Distance correction (-log A_o) as a function of distance for 3 local magnitude scales. At short distances, the Central U.S. and Tanzania scales have similar near-source attenuation. However, at distances greater than 100 km, the new central U.S. scale shows less attenuation than any other scale examined. Eastern North America follows the Tanzania scale.

The data that went into this study included short period and broadband waveforms obtained from the New Madrid Cooperative Seismic Network and may have been influenced by additional wave amplification effects due to the unconsolidated sediments of the Mississippi embayment (*Miao and Langston*, 2007; *Jemberie and Langston*, 2005; *Langston*, 2003b; *Bodin, et al.*, 2001). This distance attenuation relationship is appropriate for horizontal shear waves in the frequency band of 2 to 10 Hz defined by the Wood-Anderson torsion seismograph response used in correcting the waveform data to develop the scale.

These empirical results suggest that the crust and, possibly, the upper mantle of the central part of the continent is significantly different from other parts and plays a critical role in allowing seismic waves to very efficiently propagate to great distances. This qualitatively supports the well-known observation that felt areas are much larger in the central and eastern U.S. compared to the west (*Nuttli*, 1973; *Johnston and Schweig*, 1996). However, the data that go into developing a local magnitude scale is statistically diverse. Wave amplitudes depend on many source and propagation factors but are smoothed over by modeling a large data set of amplitudes. I suspect that the Mississippi embayment structure itself may bias amplitudes at closer ranges through soft sediment wave amplification. Thus, it is scientifically and practically important to understand the structure of the crust in the central

U.S. and to determine how it influences the wave propagation from source to local and regional receivers.

A good crustal model is essential for standard seismological operations like determining accurate earthquake locations and focal mechanisms as well as understanding the propagation factors important in controlling seismic wave amplitudes. Considerable work has been done in the northern part of the Mississippi embayment with seismic refraction (e.g., *Mooney, et al.*, 1983; *Catchings*, 1999) and reflection (*Nelson and Zhang*, 1991) to investigate large-scale crustal structure. These models have been very useful seismological benchmarks to use in travel time calculations and to infer geological and tectonic history of the area. However, I showed some years ago (*Langston*, 1994) that it was very difficult to use these simple crustal models to accurately predict the wavefield from earthquakes in the NMSZ. Refraction models, for example, generally consist of a few homogeneous layers with constant velocities that actually produce much more complicated waveforms than are observed from earthquakes because distinct, simple layer interfaces produce large reflections and multiples. In the case of understanding seismic waves from regional NMSZ events recorded at CCM (Cathedral Caves, MO) station, velocity gradients in the mid- and lower crust were needed to produce the observed simple waveforms. This was taken to an extreme, in a modeling sense, by a regional wave study of a large earthquake observed by the Tanzania Broad Band Experiment in 1994 (*Langston, et al.*, 2002). In that study, the timing and amplitude of a myriad of S wave phases seen in broadband regional waveforms out to distances of 800km could be accurately modeled with a simple crust consisting of a single velocity gradient and a Moho discontinuity. The simplicity of the crustal model was breathtaking and showed that the detailed amplitude behavior of regional waveforms could be deeply understood using insight from ray theory and the wave theory of head waves, critical reflections, and turning waves.

The purpose of the present research was to produce one or more vertically inhomogeneous crust and upper mantle velocity and anelastic attenuation models that faithfully reproduce the arrival times and amplitudes of observed shear wave trains. The frequency band of interest is from 0.3 to 10 Hz and the data was taken from recent M3.5 and above earthquakes in the NMSZ.

The approach to the problem of building a crustal model was to first pick a dense spatial grid of travel times from shear waves generated by two explosion experiments in the embayment. These travel times were used to create a smooth crustal model that serves as a starting point for synthetic seismogram calculations to investigate shear waves from the earthquakes. A novel structural inversion method, called "phase time inversion" (*Langston, et al.*, 2002) was to incorporate both the explosion travel time data and the arrival time data of major S wave phases seen in the earthquake data to produce a crustal model consistent with both. "Phase time inversion" was to be extended to include amplitudes of the S wave phases in an attempt to put constraints on details of the velocity and attenuation models.

This research represents a different approach to learning about the shear wave "path effect" of seismic waves from earthquakes compared to empirical phenomenological methods based on regression of peak acceleration or velocity data with distance (e.g., *Atkinson and Boore*,

2006; *Malagnini, et al.*, 2006; *Atkinson and Kaka*, 2007). Empirical methods are different than producing wave propagation models in that a very simple relationship is found between multiplicative factors that represent the source, path, and site characteristic of seismic ground motion that ultimately fold back into an over simplified convolutional model of wave propagation of a direct S wave. Although simplicity does have its virtues, variation of the observed amplitudes become the "error" of fit and the uncertainty in the calculation even though it is tacitly accepted that the wave propagation and source description may be arbitrarily complex and that amplitude variations may be due to sensible variations in source radiation patterns or simple wave propagation in layered media.

The strength of computational seismology is that source and structure models can be specified quite precisely so that it becomes possible to actually learn about the mechanisms of wave propagation in the earth. But this strength is also a weakness because the complexity of the wave propagation medium can easily exceed the necessary knowledge of medium parameters or characteristics needed to reproduce the seismic wave field. However, past efforts in modeling broadband seismograms at local and regional distances have been very successful in explaining the character and fine detail of observed seismograms using vertically inhomogeneous earth models (e.g., *Dreger and Helmberger*, 1990; *Helmberger, et al.*, 1992; *Langston*, 1994; *Langston, et al.*, 2002). Our hypothesis is that earthquakes recorded by the New Madrid Cooperative Seismic Network will also be amenable to analysis and will yield important information on the nature of S wave propagation in the region as well as yield new crustal model S wave velocity results that can be used in future source modeling and tomographic structure studies.

P Wave and Shear Wave Velocity Structure in the NMSZ from Explosion Data

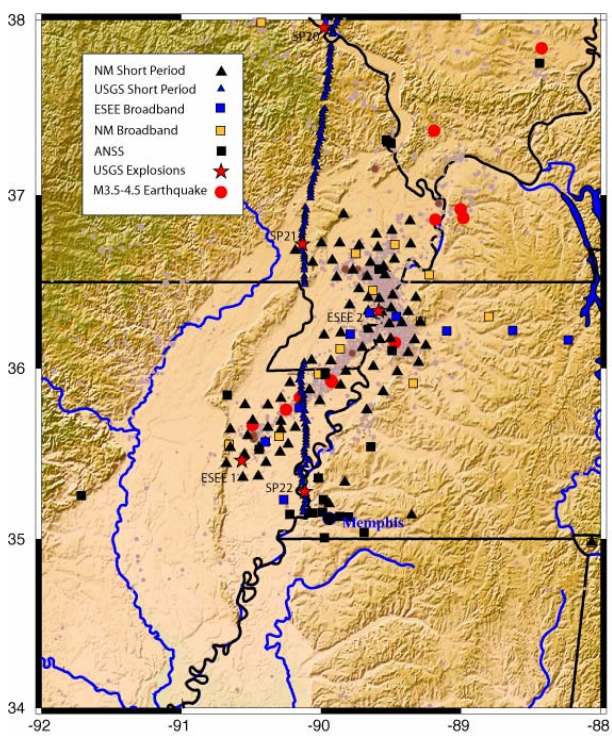

Figure 2 - Map of the area showing 10 years of earthquakes in the seismic zone, stations of the New Madrid Cooperative Seismic Network, temporary stations deployed by the 1991 USGS refraction experiment (*Catchings*, 1999), and temporary stations deployed for the 2002 Embayment Seismic Excitation Experiment (ESEE).

USGS refraction profiles from the early 1980's (*Mooney et al,* 1983) and 1990s (*Catchings*, 1999) are the basis for what's known about P and S wave velocity within the crust of the NMSZ. In a single paragraph and figure, *Catchings* (1999) gives the interpretation of S wave critical reflections from inferred interfaces in the region and also states that "there are appreciable uncertainties in picking the shear-wave refracted phase". He goes on to say that "in the absence of first-arrival shear-wave refractions, the shear-wave velocities calculated here are necessarily minimum or average velocities and are less well constrained than the P-wave velocities". As an illustration of this Figure 3 shows some of the uncertainty associated with picking phases from the explosion data.

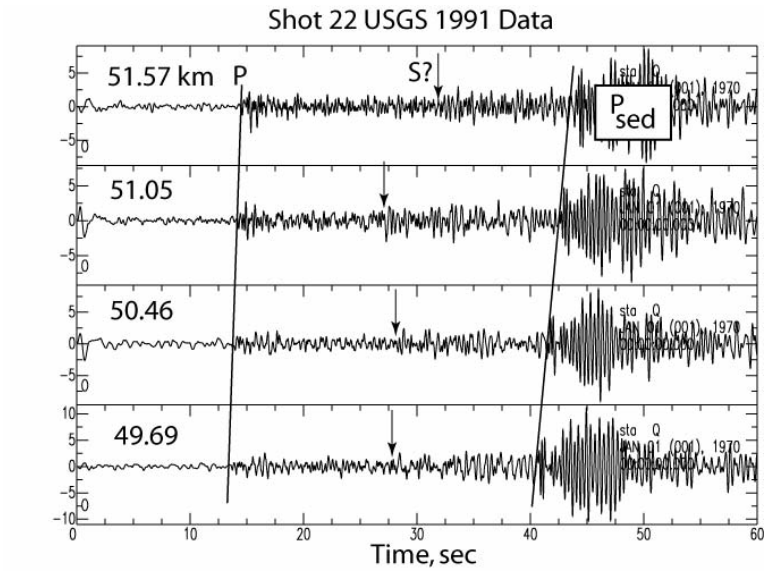

Figure 3 – Example of vertical component seismograms from the 1991 USGS refraction experiment. The source was shot 22, the southernmost large borehole explosion in the experiment (see map). These data have been filtered between 0.3 and 1.5 Hz to accentuate shear waves, if they exist. The plot shows 4 stations with large first arriving P waves and the larger trapped P wave in the unconsolidated sediment, Psed. Crustal S waves should arrive before Psed. Several possibilities are shown by the arrows.

Sources for this experiment and the later 2002 Embayment Seismic Excitation Experiment (ESEE) consisted of 50 m boreholes partially filled with fluid explosives. The 1991 dataset consists of vertical component channels only. Figure 3 shows that picking secondary arrivals in the vertical component data is difficult. This is compounded by the fact that it is well known that the unconsolidated sediments produce distinct S-to-P conversions from the Paleozoic/Tertiary boundary that, in the past, were misidentified as S waves (e.g., *Andrews, et al.*, 1985; *Chen, et al.*, 1996; *Langston*, 2003a). In 2002, the PI and Walter Mooney's Crustal Refraction group at the USGS performed a collaborative project to repeat 2 of these large borehole explosions but to record 3 component short period and broadband waveforms on the New Madrid Cooperative Seismic Network (NMCSN) as well as deploy 9 portable broadband instruments along several profiles from the explosions (Figure 2). The purpose of the experiment, ESEE, was to generate high amplitude surface waves in the embayment sediments to test for sediment anelasticity (*Langston, et al.*, 2005). It is illuminating to see how shear waves actually are manifest in the 3 component broadband data (Figure 4). Three-component data display clear S waves on both radial and transverse components of ground motion. Although the source was theoretically axisymmetric, these data show that SH waves (transverse components) were generated directly by the source or from near-source wave conversion.

Shear waves are characteristically seen in the explosion data recorded by the 3 component broadband and short period stations of the NMCSN. Shear waves are evident in the horizontal components and can be further drawn out by bandpass filtering to increase signal-to-noise ratios. Our first task was to process all available 3 component data from the two ESEE explosions, pick S wave arrivals, and make reduced traveltime plots of the waveform data to correlate arrivals over distance.

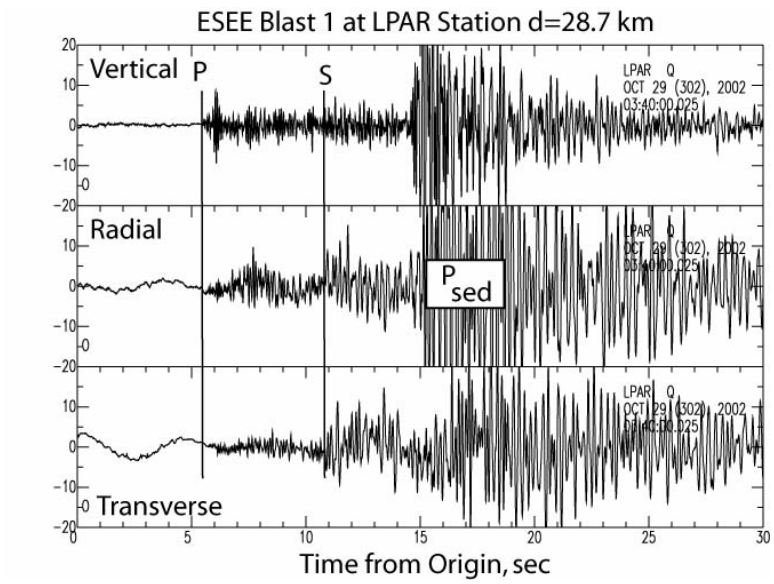

Figure 4 – 3 component raw data from LPAR station 28.7 km from the southern ESEE 2500 lb blast in 2002. Shown are vertical, radial, and transverse seismograms with P, S, and Psed waves shown. Psed is a P wavetrain trapped in the unconsolidated sediments. The horizontal components were rotated into the theoretical azimuth from the source. Note the well-defined S waves seen on the radial and transverse components arriving before Psed. Also note that it is difficult to pick the S wave on the vertical component seismogram. Compare these waveforms with those in Figure 3. S waves are unambiguous in the 3 component data.

In the following I will be referring to "blast 1" as the 2500 lb shot near Marked Tree, AR, and "blast 2" as the 5000 lb shot at Mooring, TN. Data from broadband stations were corrected to the NMCSN short-period instrument response since the bulk of the network data come from short-period stations. Converting from a broadband to a short-period response is much more possible than the other way around. The short-period system only has a dynamic range of 12 bits and is peaked near 1 Hz; its response is too narrow and the signal-to-noise ratio too high to attempt to create broadband waveforms through correction with the theoretical instrument response functions (Langston, 2003a). All data were rotated to the great circle azimuth to form radial and transverse ground motions for each source in an attempt to observe the S waves.

A pseudo record section constructed from both blasts show substantial differences for waves that propagate northward (blast 1) compared to those that propagate southward (blast 2) across the NMCSN (Figures 5 and 6). Blast 1 vertical and radial waveforms show striking S waves, particularly at distances of about 100 km and greater. S waves are more subdued for blast 2 and P and S wave amplitudes seem to decay regularly with distance (Figure 7). Distance decay of both P and S between blasts show distinct differences that are hard to understand, at first, since the ray paths through the structure should follow some kind of reciprocity. Waves from blast 1 decay quickly from the source to a distance of 100 km and then have a dramatic rise in amplitude between 100 and 150 km. Blast 2 waves generally decay monotonically with distance with the P waves decaying at a much lower rate those from blast 1. It is interesting to note that the near-source amplitude for blast 1 appears to be

larger than for blast 2 since blast 1 was half as large as 2. No source correction for source size was attempted. Nevertheless, if such a correction were applied, blast 2 data should be reduced by 0.3 units in $\log_{10}$ amplitude since blast 2 was nominally twice as large as blast 1.

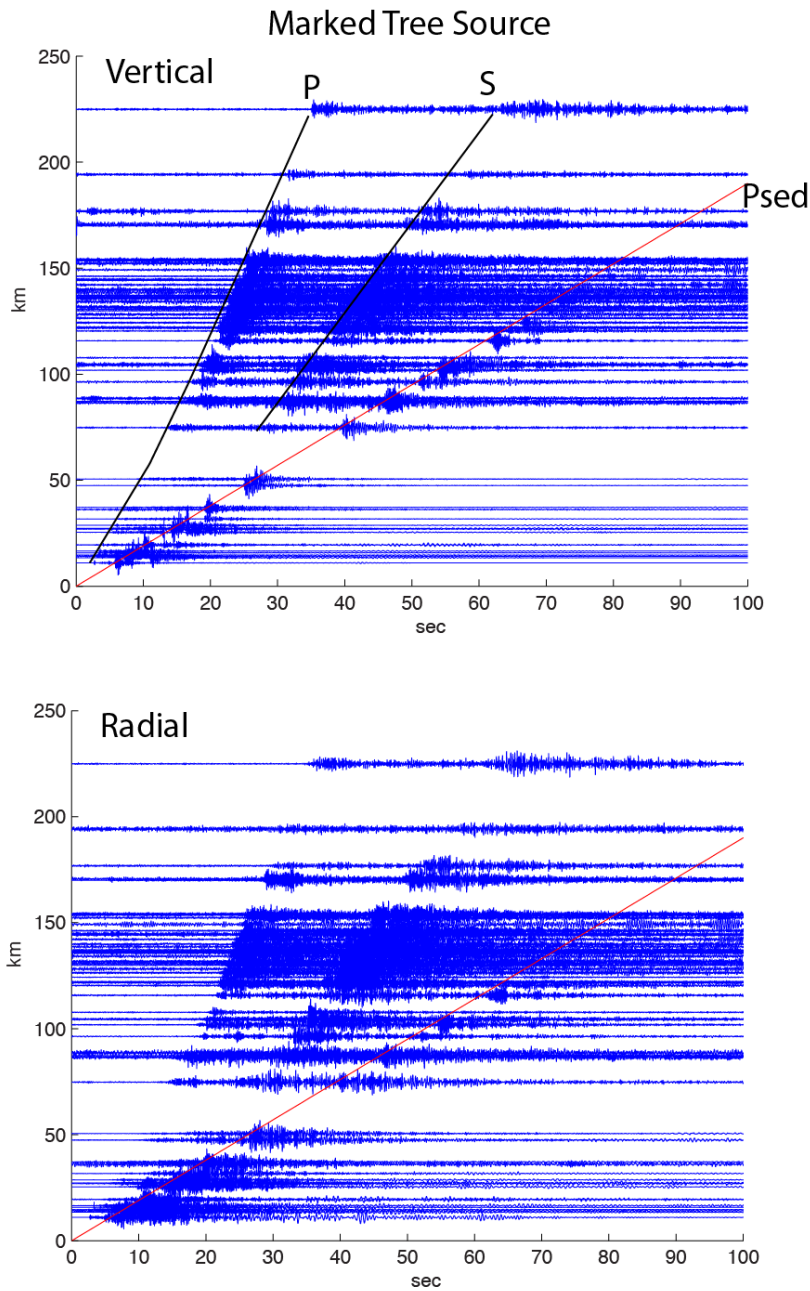

Figure 5 - Record section showing vertical and radial components of motion for the New Madrid Cooperative Seismic Network, blast 1 near Marked Tree, AR. The Psed wave is generally the largest phase on the seismogram and consists of multiply refracted and reflected P waves within the 1 to 0.7 km thick Mississippi embayment sediments. Large P and S waves appear near 100 km distance.

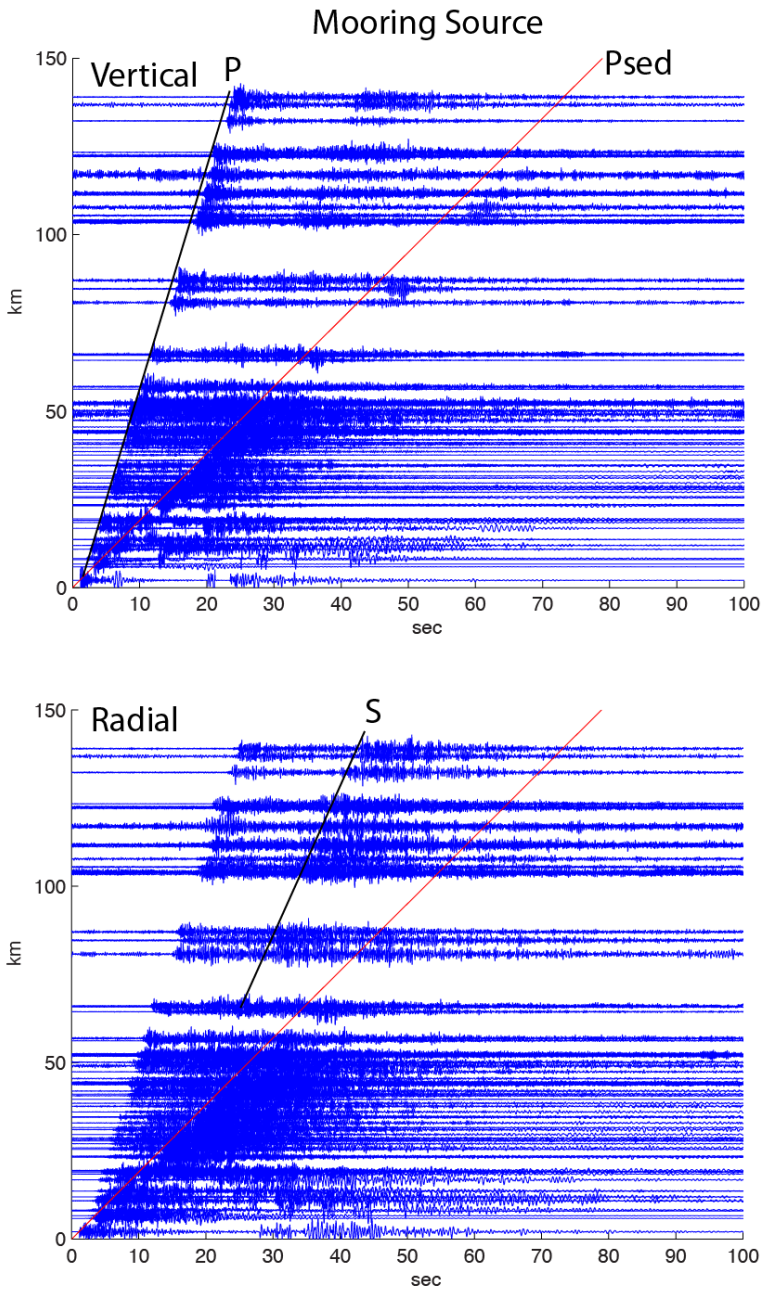

Figure 6 - Record section showing vertical and radial components of motion for the New Madrid Cooperative Seismic Network, blast 2 near Mooring, TN. The Psed wave is less prominent. P waves appear to be more homogeneous than blast 1 P waves since they have no large amplitude fluctuations with distance. S waves are less distinct but show up as emergent arrivals on the radial components.

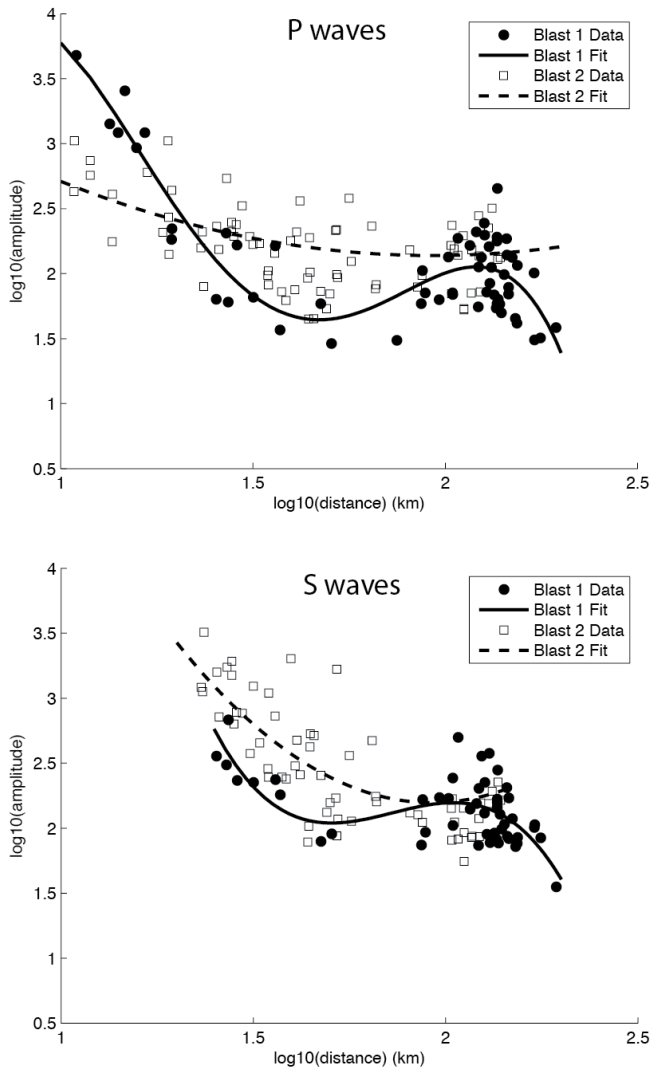

Figure 7 - Distance attenuation of short-period vertical P waves (top) and short-period radial S waves (bottom) for the data shown in Figures 5 and 6. The amplitude data were picked by removing the mean and forming the envelope function of the waveform. The maximum amplitude within a 5 second time window was picked for each seismogram and $\log_{10}$ amplitude plotted as a function of $\log_{10}$ distance. Low order polynomials were fit to the data to obtain curves shown in the figure. Note the dramatic rise in amplitude in both P and S for blast 1 near 100 km range. Blast 2 distance decay appears to be monotonically decreasing with distance.

These observations are enigmatic. They suggest that the distance decay of seismic waves is anisotropic depending on direction of propagation from the source. Considerable effort was expended in trying to reconcile these observations by looking at details of the wave propagation seen in the data. An immediate observation was that near 100 km distance, blast 1 P waves had apparent velocities of 8.2 km/s and higher but that blast 2 waves only about 6.5 km/s (Figures 8 and 9). Velocities of 8.2 km/s suggest mantle velocities, yet the nominal traveltime curve for the area based on past refraction experiments show velocities of 6.4 - 7.4 km/s, indicative of propagation in the upper crust and in the proposed "rift pillow" in the mid to lower crust (Figure 10).

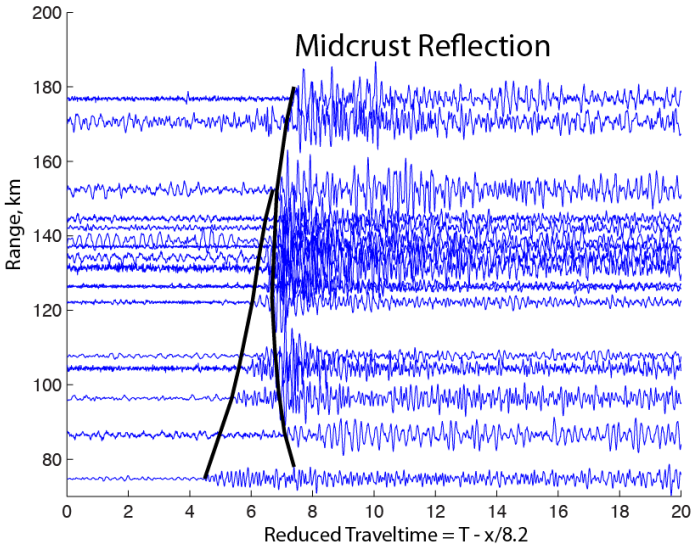

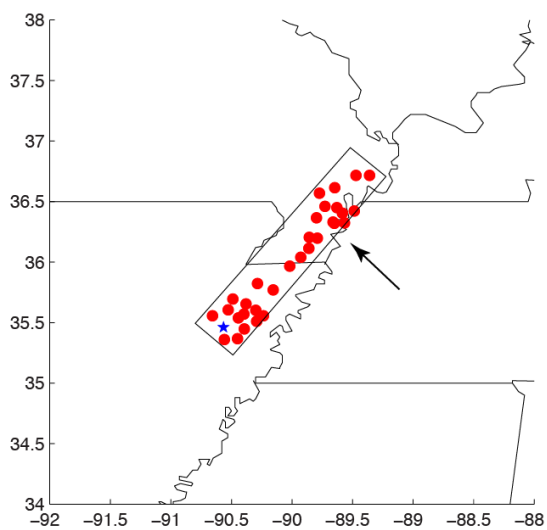

Figure 8 - Close up of vertical component data from blast 1. The data were selected in a more limited azimuthal box (shown at the bottom) to form the profile. Note that these data were reduced using a reducing velocity of 8.2 km/s. Amplitude of the large secondary arrival suggest a midcrust reflection that has gone critical with distance. The arrow shows a distance of 140 km from the source of blast 1 where the arrival has an apparent velocity of 8.2 km/s. The S wave data (not shown) shows similar behavior with a speedy 4.5 km/s apparent velocity. These large apparent velocities normally would be associated with interaction with the mantle. However, mantle cross-over is at about 200 km for the refraction models appropriate for the embayment (Figure 10). Timing suggests that this presumed reflection is from a midcrust interface. The apparent velocity must be explained by appealing to a dipping interface.

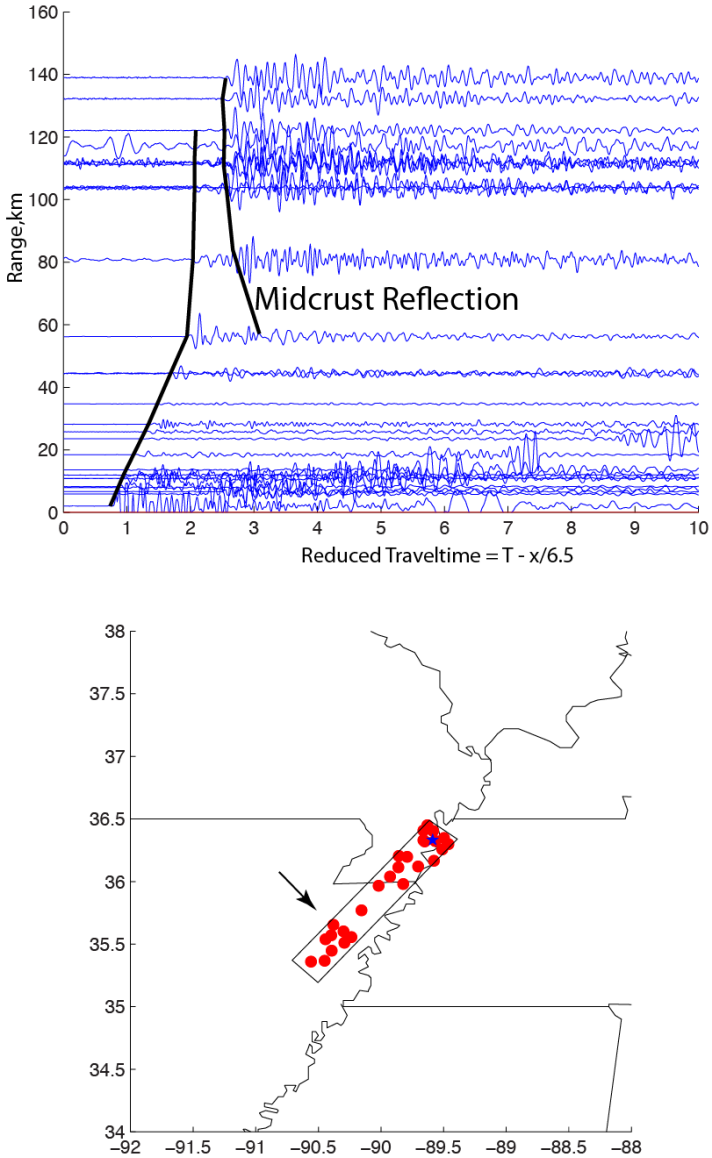

Figure 9 - Close up of vertical component data from blast 2. The data were selected in a more limited azimuthal box (shown at the bottom) to form the profile. These data were reduced using a reducing velocity of only 6.5 km/s. Amplitude of the larger secondary arrival also suggests a midcrust reflection that has gone critical with distance. The arrow shows a distance of 140 km from the source of blast 1 where the arrival has an apparent velocity of 6.5 km/s. The S wave data (not shown) shows similar behavior with a moderate 3.6 km/s apparent velocity. These apparent velocities are appropriate for the presumed midcrustal interface in the region.

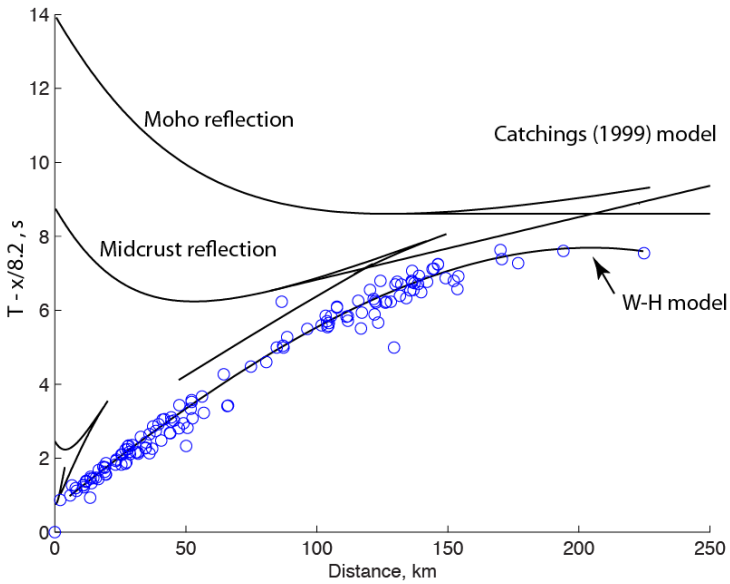

Figure 11 - Theoretical traveltime curves for P waves in Catchings (1999) model for the region. The circles are traveltime picks from all blast 1 and blast 2 data. Also shown is the traveltime for the turning wave in a model constructed using the Weichert-Herglotz technique and the observed data. Note that the observed times are 0.5 to 1 sec fast relative to the times of the Catchings (1999) model. Models are shown in Figure 12.

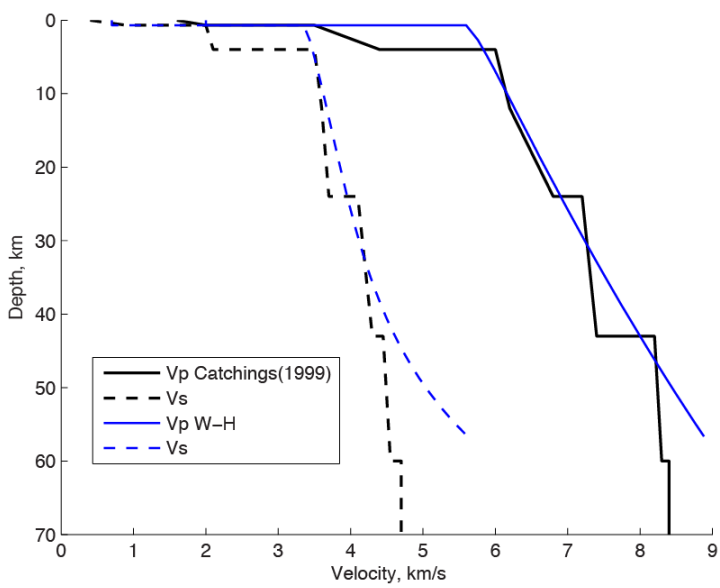

Figure 12 - Model developed from Catchings (1999) for the crust and mantle in the vicinity of blasts 1 and 2. Also shown is the smooth Weichert-Herglotz model determined from the blast traveltime data. The data appear to be 0.5 to 1 sec fast relative to the Catchings model primarily due to the relative low velocity sediments in the upper 4 km. These are due to sedimentary rift fill in the Reelfoot rift. The traveltime data do not seem to require this part of the model.

To summarize the observations, high amplitude P and S waves are observed at about 140 km distance from each source. Apparent velocity for the P wave traveling in northerly azimuths is 8.2 km/s at 140 km and, if interpreted as a post critical reflection, amplitudes appear to get large at about 100 km suggesting the occurrence of critical angle at that distance. P waves traveling south only attain apparent velocities of 6.5 km/sec at 140 km with an interpretation of critical angle occurring at 80 km from the increase in amplitude.

These observations can be reconciled with a dipping interface model where the upper crust thickens to the south by 10 km over a distance of 70 km at the expense of the lower crust, "rift pillow" structure (Figures 13 and 14). Ray tracing in such a model shows that traveltimes are nearly identical for southerly or northerly propagating P and S waves but that the apparent velocities are significantly different. Reflected waves from the dipping section of the interface are reflected up at a smaller surface incidence angle consistent with the observation of high apparent velocities. Furthermore, these reflections are post-critical and will be high amplitude. Reflected waves propagating southward encounter the dipping interface from the opposite direction so that reflections tend to flatten out, decreasing the apparent velocity. Even so, critical angles are reached at shorter distances because of the flattening of the ray path and reflections will tend to be high amplitude for greater distances. The dip of this interface is approximately 8°, which is quite large.

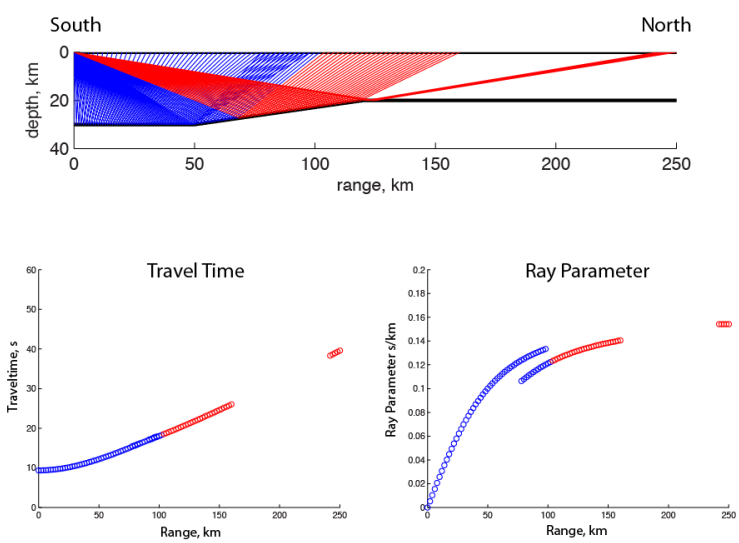

Figure 13 - Ray tracing model that conceptually explains the amplitude and apparent velocity data for blast 1. Reflection from a dipping interface dipping to the South causing lower incidence angles at the surface and high apparent velocity. The apparent velocity at 140 km is 8.2 km/s, consistent with the data. Furthermore, the observed position of the first critical angle is at 100 km, also consistent with the data. The color blue denotes rays that have precritical interactions with the interface and red, postcritical interactions. SV and SH waves, in particular, will be totally reflected in the postcritical regime, causing high wave amplitudes.

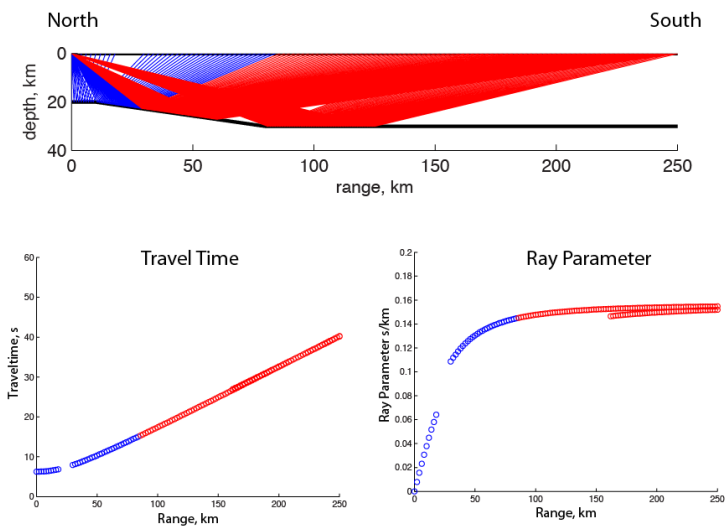

Figure 14 - Ray tracing model that conceptually explains the amplitude and apparent velocity data for blast 2. The model is identical to that shown in Figure 13. Reflection from a dipping interface dipping to the South causes higher incidence angles at the surface and low apparent velocity. The apparent velocity at 140 km is 6.5 km/s, consistent with the data. Large amplitudes for the reflection occur over a longer range since critical angles are attained at closer range. Color scheme is the same as for Figure 13.

Implications for Distance Attenuation and Synthetic Seismogram Computations

This model explains the general behavior of the amplitude, time, and apparent velocity data from the two blasts. It is remarkable that there are such differences in the wave propagation simply by reversing the azimuth of the wave propagation. Although the data yield well-determined systematics in distance attenuation for P and S wavetrains, a detailed analysis of geometrical spreading effects, anelasticity and wave propagation mechanism require the use of 2D and 3D wave propagation codes to decipher the signals. The usual heuristic explanations of a simple attenuating shear wave with distance is inadequate to the task since there is clearly more than one phase involved in wave propagation as a function of distance. Amplitude will depend on details of the velocity structure since a variety of direct, turning and reflected waves are involved, all interacting with heterogeneous structure.

These results imply that it may be misleading to use models of plane layered structure to explain the waveform data, particularly if sparse data sets are only available. This was the primary reason for limiting the analysis of the waveform data to ray tracing since 2D and 3D wave propagation codes were not available for use.

Finally, it is interesting to note that the dipping structure discovered in the explosion data is reasonably consistent with large inferred changes in the thickness of the "rift pillow" compiled by Hildenbrand (Figure 15). The explosion data recorded by the permanent

network show that it is possible to infer structure through a careful analysis of the waveforms. These data also suggest that controlled experiments may offer the best chance of learning about the first order effects of heterogeneous velocity structure on distance attenuation of seismic waves.

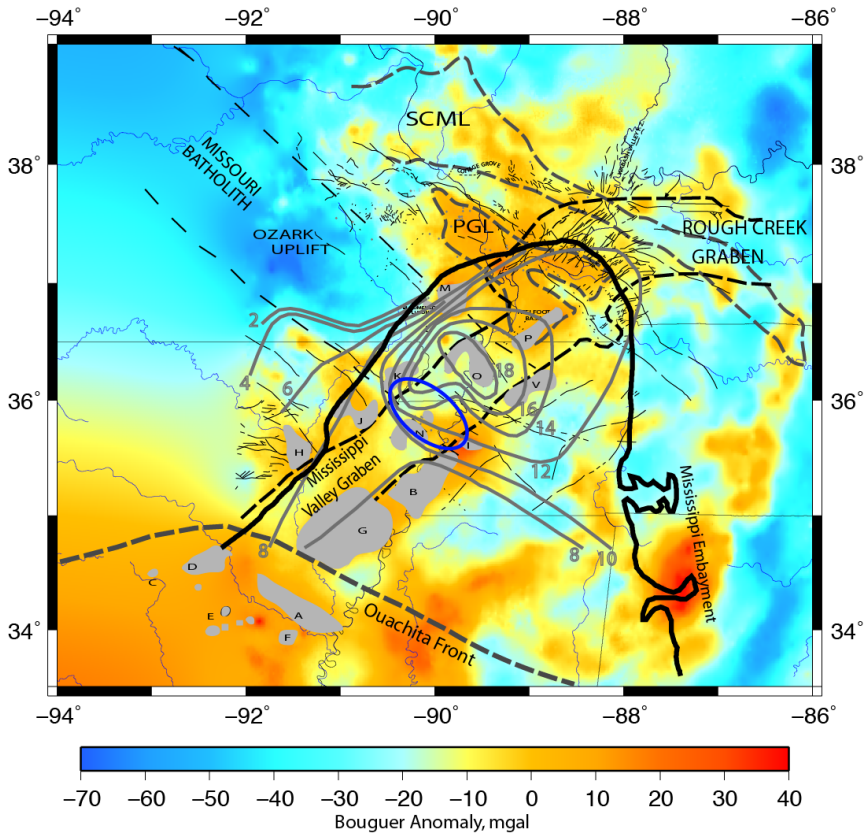

Figure 15 - Map of Bouguer gravity anomalies, the outline of the Mississippi embayment (dark line), Ouachita front and Rough Creek Graben (dotted lines) and other geophysical features in the New Madrid area. The grey lines show contours of rift pillow thickness compiled from various source by Hildenbrand (1985). The blue ellipse is the location of the dipping interface inferred from the explosion data. It occurs in the area where the rift pillow is inferred to thin dramatically.

DISPOSITION OF DATA SETS

The terms of this grant requires that all data be made freely available to other investigators. All data are available by request. The broadband data are available at the IRIS data center.

BIBLIOGRAPHY OF ALL PUBLICATIONS RESULTING FROM THIS PROJECT

None at this time. A paper is currently being prepared.

ACKNOWLEDGMENTS

CERI graduate student Mehari Ayele assisted in preparing the explosion data for analysis and is acknowledged for his help.

References

Andrews, M. C., W. D. Mooney, and R. P. Meyer (1985). The relocation of microearthquakes in the northern Mississippi embayment, *Jour. Geophys. Res.*, *90*, 10223-10236.

Atkinson, G. M., and D. M. Boore (2006). Earthquake ground-motion prediction equations for eastern North America, *Bull. Seism. Soc. Am.*, *96*, 2181-2205.

Atkinson, G. M., and S. I. Kaka (2007). Relationships between felt intensity and instrumental ground motion in the central United States and California, *Bull. Seism. Soc. Am.*, *97*, 497-510.

Bodin, P., K. Smith, S. Horton, and H. Hwang (2001). Microtremor observations of deep sediment resonance in metropolitan Memphis, Tennessee, *Engin. Geol.*, *62*, 159-168.

Catchings, R. D. (1999). Regional Vp, Vs, Vp/Vs and Poisson's ratios across earthquake source zones from Memphis, TN, to St. Louis, MO, *Bull. Seism. Soc. Am.*, *89*, 1591-1605.

Chen, K., J. Chiu, and Y. Yang (1996). Shear-wave velocity of the sedimentary basin in the upper Mississippi embayment using S-to-P converted waves, *Bull. Seism. Soc. Am.*, *86*, 848-856.

Dreger, D. S., and D. V. Helmberger (1990). Broadband modeling of local earthquakes, *Bull. Seism. Soc. Am.*, *80*, 1162-1179.

Helmberger, D. V., R. Stead, P. Ho-Liu, and D. Dreger (1992). Broadband modeling of regional seismograms: Imperial Valley to Pasadena, *Geophys. J. Int.*, *110*, 42-54.

Hildenbrand, T.G., Rift structure of the northern Mississippi Embayment from the analysis of gravity and magnetic data, *Jour. Geophys. Res*., 90, 12,607-12,622 (1985).

Horton, S. P., W.-Y. Kim, and M. Withers (2005). The 6 June 2003 Bardwell, Kentucky, earthquake sequence: evidence for a locally perturbed stress field in the Mississippi embayment, *Bull. Seism. Soc. Am.*, *95*, 431-445.

Hutton, L. K., and D. M. Boore (1987). The ML scale in southern California, *Bull. Seism. Soc. Am.*, *77*, 2074-2094.

Jemberie, A. L., and C. A. Langston (2005). Site amplification, scattering, and intrinsic attenuation in the Mississippi embayment from coda waves, *Bull. Seism. Soc. Am.*, *95*, 1716-1730.

Johnson, G. A., S. P. Horton, M. M. Withers, R. T. Cox (2008). Earthquake focal mechanisms fro the New Madrid seismic zone, *SRL, 79*, #2, 350.

Johnston, A. C., and E. S. Schweig (1996). The enigma of the New Madrid earthquakes of 1811-1812, *Annu. Rev. Earth. Planet. Sci.*, *24*, 339-384.

Kim, W.-Y. (1998). The ML scale in eastern North America, *Bull. Seism. Soc. Am., 88,* 935-951.

Kramer, S. L. (1996). *Geotechnical Earthquake Engineering*, Prentice Hall, Upper Saddle River, New Jersey.

Langston, C. A. (1994). An integrated study of crustal structure and regional wave propagation for southeastern Missouri, *Bull. Seism. Soc. Am.*, *84*, 105-118.

Langston, C. A. (2003a). Local Earthquake Wave Propagation Through Mississippi Embayment Sediments: I. Body Wave Phases and Local Site Responses, *Bull. Seism. Soc. Am.*, *93*, 2664-2684.

Langston, C. A. (2003b). Local earthquake wave propagation through Mississippi embayment sediments: II. Influence of local site velocity structure on Qp-Qs determinations, *Bull. Seism. Soc. Am.*, *93*, 2685-2702.

Langston, C. A., P. Bodin, C. Powell, M. Withers, S. Horton, and W. Mooney (2005). Bulk sediment Qp and Qs in the Mississippi embayment, Central U.S., *Bull. Seism. Soc. Am.*, *95*, 2162-2179.

Langston, C. A., A. A. Nyblade, and T. J. Owens (2002). Regional wave propagation in Tanzania, East Africa, *Jour. Geophys. Res.*, *107*.

Malagnini, L., P. Bodin, K. Mayeda, and A. Akinci (2006). Unbiased moment-rate spectra and absolute site effects in the Kachchh basin, India, from the analysis of the aftershocks of the 2001 Mw 7.6 Bhuj earthquake, *Bull. Seism. Soc. Am.*, *96*, 456-466.

Miao, Q., and C. A. Langston (2007). Empirical distance attenuation and the local magnitude scale for the central U.S., *Bull. Seism. Soc. Am.*, preprint.

Mooney, W. D., M. C. Andrews, A. Ginzburg, D. A. Peters, and R. M. Hamilton (1983). Crustal structure of the northern Mississippi embayment and a comparison with other continental rift zones, *Tectonophysics*, *94*, 327-348.

Nelson, K. D., and J. Zhang (1991). A COCORP deep reflection profile across the buried Reelfoot rift, south-central United States, *Tectonophysics*, *197*, 271-293.

Nuttli, O. W. (1973). The Mississippi Valley earthquakes of 1811 and 1812: intensities, ground motions, and magnitudes, *Bull. Seismol. Soc. Am.*, *63*, 227-248.

Zhao, M., C. A. Langston, A. A. Nyblade, and T. J. Owens (1999). Upper mantle structure beneath southern Africa, *J. Geophys. Res.*, *104, 4783-4794*.